Utilising Nonlinear Air Damping as a Soft Mechanical Stopper for MEMS Vibration Energy Harvesting

Utilising Nonlinear Air Damping as a Soft Mechanical Stopper for MEMS Vibration Energy Harvesting

Shao-Tuan Chen[1], Sijun Du[1], Emmanuelle Arroyo[1], Yu Jia[1,2] and Ashwin Seshia[1]

[1] Nanoscience Centre, University of Cambridge, Cambridge, CB3 0FF, UK
[2] Department of Mechanical Engineering, University of Chester, Chester CH1 4BJ, UK
E-mail: **stc33@cam.ac.uk**

Abstract. This paper reports on the theory and experimental verification of utilising air damping as a soft stopper mechanism for piezoelectric vibration energy harvesting to enhance shock resistance. Experiments to characterise device responsiveness under various vibration conditions were performed at different air pressure levels, and a dimensionless model was constructed with nonlinear damping terms included to model PVEH response. The relationship between the quadratic damping coefficient ζ_n and air pressure is empirically established, and an optimal pressure level is calculated to trade off harvestable energy and device robustness for specific environmental conditions.

1. Introduction

Microelectromechanical systems (MEMS) technology has enabled the construction of chip-scale vibration energy harvesters with the potential for close in-package or monolithic co-integration with standard CMOS technology. Despite the demonstration of useful power output from MEMS vibration energy harvesters [1], the lack of robustness of MEMS devices due to the brittleness of silicon has hindered commercialisation and real-world application, as large amplitude vibrations in operational environments often cause cantilevered MEMS devices to fracture [2], as shown in Fig.1. Nonlinear air damping has been observed by Jia et al. [3] when the PVEH operates under atmospheric conditions, which limits the maximum displacement of the PVEH when subjected to large amplitude excitation. While this effect reduces the overall power output, it can also serve as a 'soft' mechanical stopper to constrain the vibration amplitude of the harvester. This in turn helps the harvesters to survive at high acceleration levels whereas PVEHs operating in vacuum environments fracture due to excessive displacement under identical drive conditions. Therefore, nonlinear air damping can potentially serve as a soft stopper and prevent devices from failure due to shock or other excessive dynamic loading.

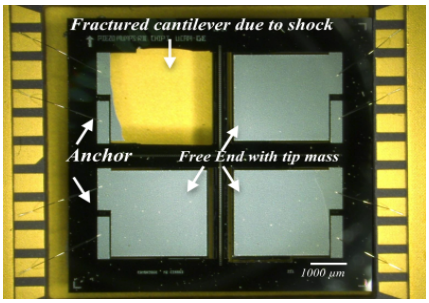

Figure 1. Picture of MEMS PVEH [1] The top left corner reveals fractured PVEH due to shock excitation.

2. Nonlinear model

This paper investigates the variation of maximum power output by PVEH with varying air pressure inside the MEMS package. The PVEH is designed by Jia et al. [3] as a cantilever with proof mass at the free end. The dimensions of the cantilever are 3.5mm by 3.5mm, and the proof mass is comprised

of an un-etched silicon substrate (400 μm). The particular device considered in this study has a proof mass to cantilever length ratio of 70%.

A dimensionless model was constructed with nonlinear damping to analytically model the time response of the cantilever and to verify the effect of air damping ζ_n on the displacement of the MEMS PVEH. Nonlinear dissipation of vibrating cantilevers can have several origins, such as geometric nonlinearities or viscous damping by the ambient medium. The equation of motion with nonlinear damping has been previously investigated by Ravindra [4] on soft Duffing oscillators, with the nonlinear damping term taken to be proportional to the pth power of the velocity of the system, in the form of :

$$a_p \dot{x}|\dot{x}|^{p-1} \tag{1}$$

where $p \geq 1$ is the nonlinear damping exponent, and α_p is the corresponding damping coefficient.

The precise value for the nonlinear damping exponent can be determined by considering the physical origin of the damping effect. For MEMS devices operating in air, the cantilever is oscillating in a fluid, and the fluid drag force accounts for the nonlinear air damping effect in the physical model. The amplitude of the fluid drag force can be expressed as a quadratic function of velocity [5]. As a result, the response of a PVEH oscillating in air is modelled by a nonlinear-damped Duffing equation with a quadratic damping term as:

$$\ddot{x} + 2\zeta w_n \dot{x} + \zeta_n \dot{x}|\dot{x}| + \mu x^3 + {w_n}^2 x = A w^2 \cos(wt) \tag{2}$$

where x is the displacement, ζ is the viscous damping, ζ_n is the quadratic damping representing nonlinear air drag, μ is the Duffing coefficient, w_n is the natural frequency, A is the excitation displacement amplitude, w is the excitation frequency and t is the time domain.

The maximum displacement of the cantilever in air as a function of the nonlinear air damping coefficient ζ_n can be numerically obtained through the dimensionless model, and is shown in Fig.2. As seen from the figure, the maximum displacement flattens off and amplitude saturation is observed as the excitation increases with higher nonlinear air damping.

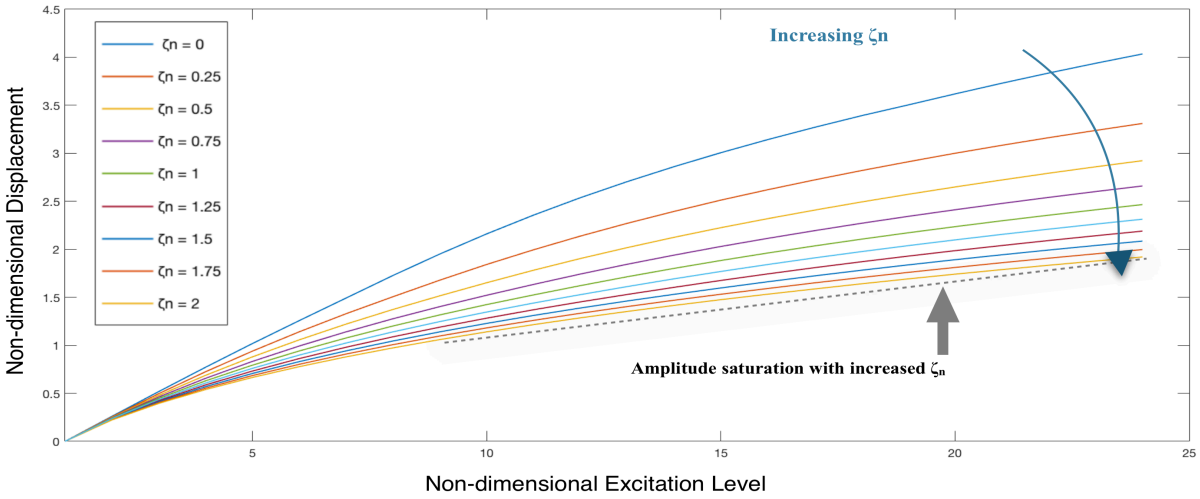

Figure 2. Dimensionless model demonstrating excitation-displacement relationship for various values of nonlinear air damping ζ_n. As ζ_n increases, amplitude saturation is observed

3. Experimental characterisation

3.1 Experimental setup

Characterisation experiments are performed to obtain the relationship between output power and input excitation for the PVEH with different air pressure levels. The experimental apparatus is shown in Fig. 3. The PVEH is inserted onto a chip carrier, mounted to a shaker with a custom PCB, and the entire setup is placed in a vacuum chamber, evacuated using a vacuum pump to adjust the air pressure level inside the chamber. Sinusoidal excitation operating at the device resonance frequency with mean amplitude varying from 0.5 to 10 g is supplied to the PVEH via a function generator (Agilent 33220A), and the operating air pressure is set to be 1, 3, 10, 200, 500 and 1000 mbar, respectively.

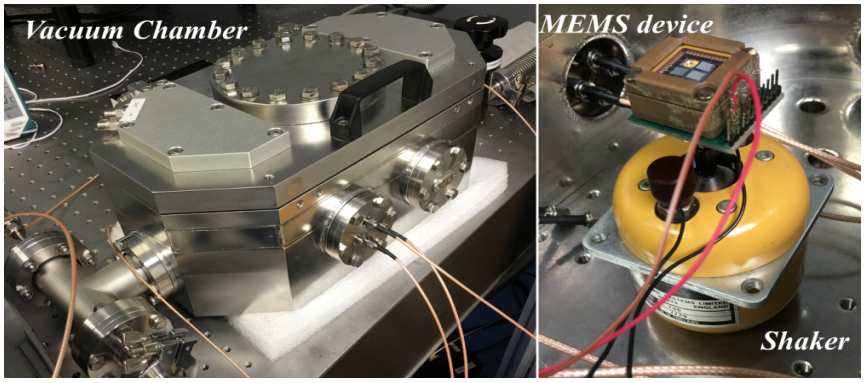

Figure 3. Experimental setup.

3.2 Sinusoidal excitation

The maximum power output of the PVEH under varying excitation levels recorded at different air pressure levels is shown in Fig.4. For larger excitations, lower air pressure cases have steeper slope between excitation and power output, whereas the slope decreases as air pressure increases. This is due to the diminishing displacement of the PVEH due to nonlinear damping, which results in the device describing amplitude saturation.

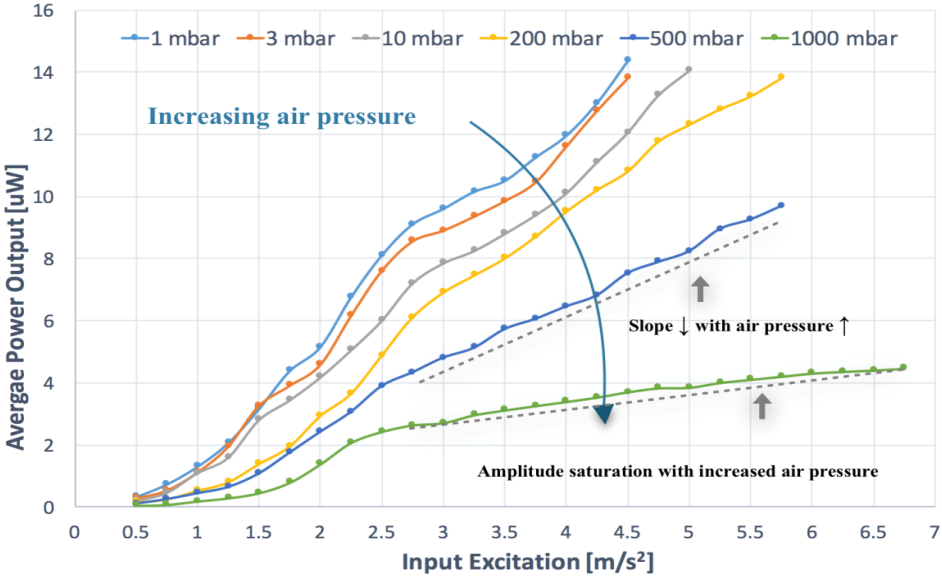

Figure 4. Excitation-Power output curve with sinusoidal excitation.

3.3 Parameters extraction

The relationship between power output under different air pressure levels and the quadratic damping coefficient in the nonlinear Duffing model can be established by nonlinear curve fitting using the Levenberg-Marquardt (LM) algorithm, described in [6]. The linear parameters of the cantilever in this study are measured and reported in [3]. The nonlinear duffing stiffness μ is derived from the experimental results at 1 mbar, considering the effect of nonlinear damping in rarefied regime negligible [7]. The parameters of the cantilever are listed in Table 1.

Table 1. Parameters of the PVEH

	w_n	ζ	μ
Value	215	0.0035	3.02×10^{-4}
Unit	Hz	1/s	N/m

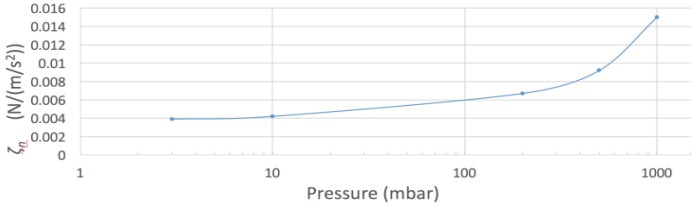

Fig.5 Quadratic damping coefficient VS air pressure

Fig.5 demonstrates the relationship between quadratic damping coefficient and air pressure level by fitting the excitation-power output response of the cantilever using the LM algorithm. As seen from the figure, the quadratic damping coefficient increases as the ambient pressure in the vacuum chamber increases, which in turn reduces the maximum displacement of PVEH for the same excitation level conditions.

3.4 Random vibration testing

Apart from the sinusoidal resonant response, Fig.6 further compares the average power output for PVEH under different air pressure subjecting to band-limited white noise vibration. Random excitation experiments are performed with band-limited white noise vibration input (10 Hz to 2 kHz) under varying air pressure from 1 to 1000 mbar to validate utilising nonlinear damping as a soft stopper.

Fig.6 (a) illustrates the time response of the cantilever when subjected to 7 g of band-limited white noise (0.025 g^2Hz^{-1}). The average power response for different air pressure were 76.63 nW, 64.48 nW, 35.07 nW, 28.85 nW and 13.39 nW, for air pressure at 1 mbar, 3 mbar, 10 mbar, 200 mbar, 500 mbar and 1000 mbar respectively, as shown in Fig.6 (b). The experiment demonstrates that increasing air pressure level can effectively reduce the maximum displacement of PVEH, reducing the impact of high frequency shock in a stochastic excitation scenario, which prevents onset of failure by fracturing and serves as a protective soft stopper for PVEH employed in harsh environments.

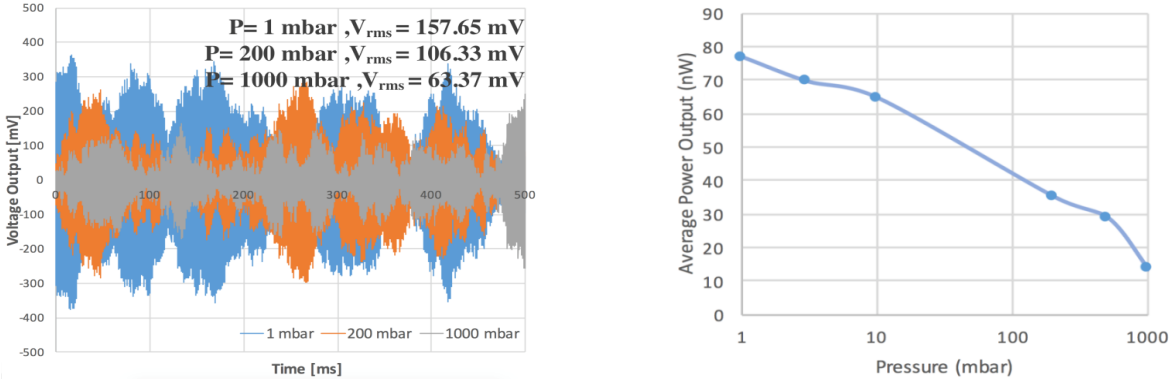

Figure 6(a) & (b). (a) Response of PVEH driven by random excitation with 0.15 g ,1000 Hz band-limited white noise. (b)Average power output with varying air pressure. When pressure increased, the output voltage diminished from 76.63 nW to 13.39nW, verifying air damping as soft stopper for random excitation environment

4. Design Guidelines

In order to prevent device from fracturing, the failure limit in terms of maximum displacement of PVEH is derived based on the fracture strength of silicon and PVEH geometry.

For a simple rectangular cantilever with length l subjecting to base excitation, the static maximum stress and deflection of the cantilever can be derived with Euler-Bernoulli beam equation [8]. However, in dynamic loading scenarios, the deflection and stress fluctuates with time, also nonlinear stiffness and damping of the cantilever contribute to the system dynamics.

If a sinusoidal excitation $P=Aw^2cos(wt)$ with amplitude $|Aw^2|$ is applied to the cantilever, the maximum deflection δ_l under different excitation amplitudes and air pressure levels can be solved numerically with the value of both linear and nonlinear parameters derived from prior experimental characterisation of the devices. The time response of the cantilever with nonlinear air damping is described in Eqn. 2, where $|Aw^2|$ is the amplitude of the fluctuating load, and x is the deflection of the cantilever.

Also under dynamic loading, the maximum bending stress of the cantilever as a function of maximum deflection of the cantilever can be approximated as [9]:

$$\sigma_{max} = \frac{EI}{Z}\delta''(0) = \frac{3EI}{Z}\frac{\delta_l}{l^2} \tag{3}$$

where E is the Young's Modulus of the cantilever, I is the moment of inertia and Z is the section modulus of the cantilever. As seen from Eqn. 3, the bending stress is a function of maximum deflection of the cantilever when it is subjected to dynamic loading. The failure limit is then defined as the maximum sustainable deflection of the cantilever before the maximum bending stress reaches the fracture strength of silicon, thus for a given PVEH, the failure limit can be determined by the

geometry of the PVEH.

For a given environment, the excitation range can be defined as the maximum excitation amplitude of the cantilever before the cantilever reaches the failure limit. Based on the dimensionless model, the excitation range can be expressed as a function of nonlinear damping ζ_n when the failure limit is known, as shown in Fig.7. As seen from the graph, for the same excitation level, as nonlinear damping increases, the deflection of the cantilever decreases. As a result, the excitation range for the device can be extended as nonlinear damping is increased, meaning the device with higher nonlinear damping can be employed into environment with higher excitation range without the device reaching the maximum deflection and fractures with excessive dynamic stress.

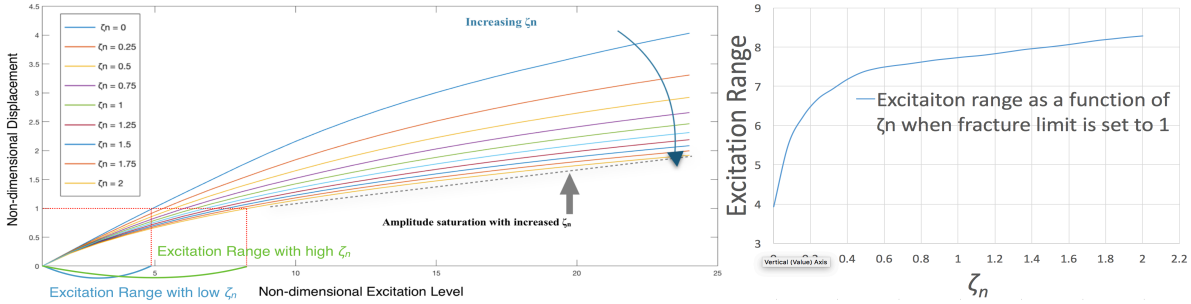

Figure 7(a)&(b). Schematic of (a) relationship between excitation range with nonlinear damping when the failure limit of PVEH is set to be 1 (b) Excitation range as function of ζn in the range between 0 to 2 calculated with the dimensionless model when the failure limit of PVEH is set to be 1, and failure limit of a PVEH based on the geometry of the device and fracture strength of silicon

5. Conclusion and Future work

While vacuum packaging is typically used in MEMS applications to minimise air damping, this paper presents a novel application of utilising air damping as a soft stopper for PVEHs. The results show that the excitation-power characteristic of the PVEH can be altered by varying the air pressure level. For larger excitation, higher air pressure reduces the power output of the PVEH, and the bounded PVEH displacement can prevent device failure by fracturing. As a result, the device is able to withstand higher excitation level before reaching the failure limit with higher air pressure, thus the range of input excitation can be extended at higher pressures, facilitating suitability for deployment in high excitation environments. The failure limit and excitation range of a rectangular cantilever with air damping subjecting to sinusoidal excitation is demonstrated in this study, as future work aims to calculate the optimized level of nonlinear damping based on device fracture limits and the excitation condition for a given device and deployment environment.

References:

[1] Cook-Chennault K, Thambi N, and Sastry AM 2008 *Smart Materials and Structures* **17(4)** p. 043001.
[2] Wang Z, Elfrink R, Rovers M, Matova S, van Schaijk R and Renaud M 2014 *Journal of Microelectromechanical Systems* **23(3)** p. 539-548.
[3] Jia Y and Seshia A A 2016 *Journal of Microelectromechanical Systems* **25(1)** p. 108-117.
[4] Ravindra B and Mallik A K 1994 *Physical Review E* **49(6)** p. 4950-4954.
[5] Hoerner S F 1965 *Fluid-dynamic drag: practical information on aerodynamic drag and hydrodynamic resistance*, Hoerner Fluid Dynamics.
[6] Lourakis M A 2005 *Foundation of Research and Technology* **4** p. 1-6.
[7] Sumali H 2007 *Journal of Micromechanics and Microengineering* **17(11)** p. 2231.
[8] Truesdell C and Noll W2004 *The non-linear field theories of mechanics*, in *The non-linear field theories of mechanics*, Springer. p. 1-579
[9] Suhir E 1997 *IEEE Transactions on Components, Packaging, and Manufacturing Technology* **20(4)** p.513-517.